A Mechanical Analysis of
Rotating-Coil Magnetometers

S. Sorti[1,2], C. Petrone[2], S. Russenschuck[2], F. Braghin[1]

[1]*Politecnico di Milano, Department of Mechanical Engineering, Via La Masa, 1, 20156, Milano,
Italy, stefano.sorti@polimi.it, francesco.braghin@polimi.it*
[2]*European Organization for Nuclear Research 1205 Geneva, Switzerland, 1211 Meyrin,
Switzerland, carlo.petrone@cern.ch, stephan.russenschuck@cern.ch*

Abstract – **Rotating-coil magnetometers are among the most common and most accurate transducers for measuring the integral magnetic-field harmonics in accelerator magnets. The measurement uncertainty depends on the mechanical properties of the shafts, bearings, drive systems, and supports. In this paper we study the mechanical phenomena (static and dynamic) affecting rotating-coil measurements and propose analysis and diagnostic methods for improving the instrument in terms of material choice and geometrical design.**

The propagation of uncertainty is investigated on the measured quantities (induced voltages, integrated and developed into a Fourier series, the coefficients of which are know as field harmonics). This results in a consistent framework for the design of a measurement bench for rotating-coil magnetometers. The paper also presents the design of a complete system, including displacement stages, supports, rotating coils, and an angular position system.

I. INTRODUCTION

Rotating-coil systems are a special form of induction-coil magnetometers, making use of Faraday's law of induction. They are applied to measuring integral field harmonics in the magnet bore, using coils mounted on a rotating shaft that is aligned with the magnet axis. A voltage is thus induced, directly proportional to the flux linkage with the coil. Typically, one long coil (or a chain of shorter coils) spans the entire magnet, including the fringe-field areas, because the transversal, integrated field is often sufficient for beam tracking in particle accelerators [1].

Precise measurements of magnetic fields rely on the mechanical properties of the benches and the rotating coils, subject to static and dynamic forces. This requires control of mechanical properties [2] and the evaluation of vibrations [3]. Typically, a shaft is designed to have natural frequencies higher than the operating frequencies [4]. Additionally, compensation schemes for the main field harmonic, commonly referred to as *bucking*, provide an effective mitigation of spurious field harmonics due these vibrations [5].

An analytical model for the mechanical description of rotating-coils was proposed in [6]. This model can predict the effect of static coil deformations, coil-axis to magnet alignment tolerances, and vibration modes on the measured field harmonics. The model suffers, however, from intrinsic limitations, mainly because axial and torsional dynamics are not explicitly considered and the shaft is modeled as a single, homogeneous, straight beam on two end supports. Although these aspects can be partially overcome by expanding the analytical model [7], a mathematical optimization of the shaft often requires numerical simulations of complex geometries with different material combinations. Therefore, this paper proposes a finite-element formulation (FEM), suitable to include more complicated coil geometries and shaft.

Improving the insight of how the mechanical design and properties affect the measured quantities is particularly important for slim shafts and/or moving systems. The realization of a versatile rotating-coil system at CERN is the first tangible outcome of this study.

II. THE MAGNETO-MECHANICAL MODEL

A 3D FEM is proposed to describe rotating-coil shafts and their supporting structures. The resulting mechanical deformation field $\mathbf{u}(\mathbf{r})$ (where $\mathbf{u}$ is the displacement vector and $\mathbf{r}$ the position) is applied to the coil geometry in order to evaluate its effects on the magnetic measurements. The FEM model is shown in Fig. 1.

A. The mechanical model

In the simplest case of quasi-static rotation of an axisymmetric shaft, the rotating coil and support can be modelled as directly coupled, otherwise it is more suitable to construct separate models and link them by appropriate interface conditions. This allows, if necessary, to approach the rotating coil in terms of rotordynamics [8]. The model is based on Timoshenko beams with 12 degrees of freedom (DOF) per node. Details on the implementation can be found in [10]. FEM can model also lumped masses, springs and dampers. It allows to include non-ideal boundary conditions: clamped or hinged ends can be replaced by
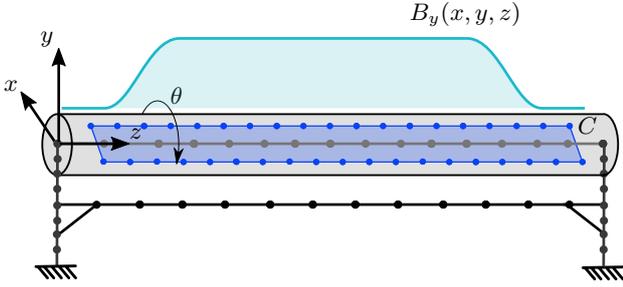
Fig. 1. A schematics of the FEM model, representing a rotating-coil system mounted on a support structure. Both shaft (light grey) and supporting structure (black) are meshed with beam elements. The induction coil is modelled as a surface that is subjected to the shaft deformation field. When the shaft rotates it will intercept a magnetic flux density whose y component is indicated.

elastic foundations with a suitable stiffness. After matrix assembly, the subset $\mathbf{z}$ of free DOFs is taken. The equation of motion is

$$M\ddot{\mathbf{z}} + R\dot{\mathbf{z}} + K\mathbf{z} = \mathbf{f}, \qquad (1)$$

where M, K and R are the mass, stiffness and damping matrices of the system. Damping is characterized experimentally as modal damping, and $\mathbf{f}$ accounts for external forces acting on the system. These include gravity, unbalancing, and vibration of moving parts. Modal transformation is applied to introduce modal coordinates $\mathbf{q}$ with $\mathbf{z} = [\Lambda]\mathbf{q}$. Rearranging equation 1 and rescaling mode to have unitary modal masses (it implies that modal mass matrix becomes the identity matrix), the mechanical model results in a state-space formulation of the form

$$\begin{pmatrix} \ddot{\mathbf{q}} \\ \dot{\mathbf{q}} \end{pmatrix} = \begin{pmatrix} -[R_{\mathrm{m}}] & -[K_{\mathrm{m}}] \\ [I] & [0] \end{pmatrix} \begin{pmatrix} \dot{\mathbf{q}} \\ \mathbf{q} \end{pmatrix} + \begin{pmatrix} [\Lambda]^T \\ [0] \end{pmatrix} \mathbf{f}, \quad (2)$$

$$\begin{pmatrix} \dot{\mathbf{z}} \\ \mathbf{z} \end{pmatrix} = \begin{pmatrix} [\Lambda] & [0] \\ [0] & [\Lambda] \end{pmatrix} \begin{pmatrix} \dot{\mathbf{q}} \\ \mathbf{q} \end{pmatrix}, \qquad (3)$$

where $[R_{\mathrm{m}}]$ is the modal damping, $[K_{\mathrm{m}}]$ the modal stiffness matrix. The second equation system described the systems response in terms of nodal displacements. Employing the FEM shape functions, the nodal displacements can be interpolated for any point of the shaft, which yields the deformation field also for the geometry of the coil. For the calculation of the magnetic flux increments, the nominal shaft rotation is expressed by the angular displacement θ. Despite the fact that this paper presents only rotating-coil applications, so $\theta = \omega t$, it is possible to model any type of induction coil. For instance, flip-coils [9].

B. The magnetic model

The mechanical model is coupled with the magnetic model, by computing the magnetic-flux linkage with the induction coil. For calculating the system's response to

a given field distribution, the magnetic flux density is expressed analytically. The typical description for integral flux density is the 2D multipoles expansion [1] but, for a correct modelling, the full 3D field is required, because integral coils intercept also magnet fringing field. Therefore, 3D pseudo-multipoles are adopted [11]:

$$B_r(r, \varphi, z) = -\mu_0 \sum_{n=1}^{\infty} r^{n-1} \Big(\overline{\mathcal{C}}_n(r, z) \sin n\varphi $$
$$+ \overline{\mathcal{D}}_n(r, z) \cos n\varphi \Big) \qquad (4)$$

$$B_\varphi(r, \varphi, z) = -\mu_0 \sum_{n=1}^{\infty} nr^{n-1} \Big(\widetilde{\mathcal{C}}_n(r, z) \cos n\varphi $$
$$- \widetilde{\mathcal{D}}_n(r, z) \sin n\varphi \Big) \qquad (5)$$

$$B_z(r, \varphi, z) = -\mu_0 \sum_{n=1}^{\infty} r^n \Big(\frac{\partial \widetilde{\mathcal{C}}_n(r, z)}{\partial z} \sin n\varphi $$
$$+ \frac{\partial \widetilde{\mathcal{D}}_n(r, z)}{\partial z} \cos n\varphi \Big) \qquad (6)$$

where

$$\overline{\mathcal{C}}_n(r, z) = n\mathcal{C}_{n,n}(z) - \frac{(n+2)\mathcal{C}_{n,n}^{(2)}(z)}{4(n+1)} r^2 + \dots \quad (7)$$

Experience shows that this series can be typically truncated after first term. Therefore, only the leading terms $n\mathcal{C}_{n,n}(z)$ are considered and expressed as

$$\mathcal{C}_{n,n}(z) = \mathcal{C}_n E(z), \qquad (8)$$

where $E(z)$ is the Enge function modelling the field roll-off in the magnet ends. The field profile is shown in Fig. 1. The flux linkage in the coils is then calculated numerically with

$$\Phi = \int_{\mathscr{A}} \mathbf{B} \cdot \mathrm{d}\mathbf{a}. \qquad (9)$$

In a discrete setting, the flux increments Φ_m for angular positions θ_m can be developed into a discrete Fourier series

$$\Psi_n = \sum_{m=0}^{M-1} \Phi_m \cdot e^{\frac{-i2\pi mn}{N}}. \qquad (10)$$

This yields the harmonic content of the systems response:

$$C_n(r_0) = r_0^{n-1} \frac{\Psi_n}{k_n}, \qquad (11)$$

where $C_n^{\mathrm{a}}(r_0) = B_n^{\mathrm{a}}(r_0) + iA_n^{\mathrm{a}}(r_0)$ are the measured (apparent) field harmonics and k_n are the coil sensitivity factors for the n-th field harmonic:

$$k_n = \frac{N_T L_c}{n} (r_2^n - r_1^n), \qquad (12)$$

where N_T is the number of coil turns, L_c the total length of the coil and the two radii are the position of the go and
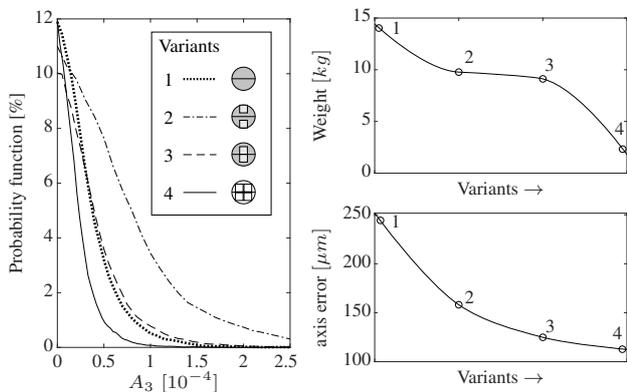
Fig. 2. Investigated shaft solutions. A bulk epoxy-resin coil; Variant 1. Square-shaped carbon-fiber tubes in different structures and dimensions; Variants 2 and 3. Full carbon-fibre shaft; Variant 4.

return wire of the coil. k_n expresses the integral sensitivity of the coil and it is therefore not function of z. The difference between the imposed A_n, B_n and the apparent A_n^a, B_n^a coefficients at the reference radius of measurement is the main figure of merit to evaluate the effects of mechanical defects.

III. THE MEASUREMENT SYSTEM

The proposed model is devoted to the design of measurement systems. Given the flexibility of the model, the design process can be simplified and generalized by separating the procedure in three steps. A rotating-coil can be designed by approximating the structure with an estimated equivalent stiffness. Then, the support can be designed for a worst-case shaft properties. Finally, the rotating-coil and the support are evaluated together.

A. Rotating-coil design

The magneto-mechanical model presented in the previous section is the basis for the shaft design. Without a loss of generality, the shaft is designed for measuring the field harmonics in a quadrupole magnet. The bucking improves the field harmonics sensitivity by compensating mechanical influences. The requirements for the coil fabrication and mounting process give a bucking ratio between 100 and 2000 (ratio between main-coil sensitivity k_A to the sensitivity of compensation scheme $k_A - k_B - k_C + k_D$). In the proposed evaluation procedure, the coil imperfections are introduced as a Gaussian distribution of the coil width (or displacements, or both effects combined), and a sample of coil sets is analysed statistically.

The external forces are gravity, support vibrations (in the form of harmonic forces on bearings), bearing-friction related torque, and shaft unbalancing due to eccentricity and sag. The excitations which do not depend upon the shaft
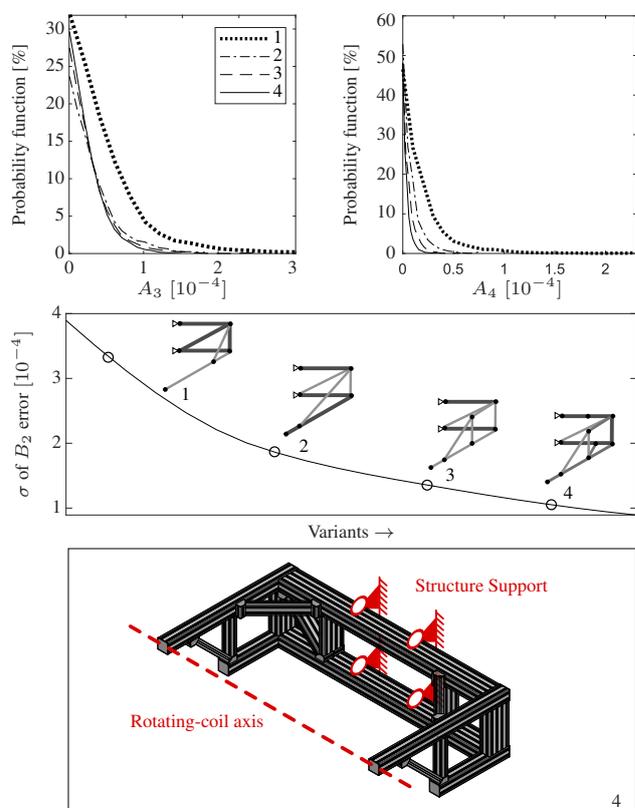

Fig. 3. A summary of the evaluation of structure solutions. The probability function of the multipole field errors A_3^a and A_4^a is plotted, together with the evolution of standard deviation of errors of the main component. The final solution is shown in more detail in the bottom part of the figure.

design (practically all, but gravity) are given in Table 1. The boundary conditions for the shaft are elastic supports (lumped springs and dampers), accounting for the equivalent stiffness of the supporting structure. This is a simplification with respect to the general case presented in Sec IIA, to speed up the design process. It is valid only if the first natural frequency of the structure is outside the range of interest (typically $0 - 30$ Hz). The designs were tested for the entire sample of bucking schemes and excitations.

As an example, different proposals for a shaft of 1.5 m length and 72 mm diameter (with a measurement reference radius of 30 mm) are evaluated, as shown in Figure 2. A bucking ratio of 100 is assumed. Measurements are

Table 1. Excitation amplitudes and directions assumed for rotating-coil design simulations

	Support vibr.	Eccentricity	Bear. friction
Ampl.	$50\ \mu m$	1 mm	0.002 mg
Dir.	$x - y$ plane	$x - y$ plane	θ dir.

simulated with the coil on the magnetic axis of a perfect quadrupole magnet. From the simulated feed-down components (A_1^a, B_1^a), the apparent axis misalignment can be calculated. Variant 4 is by a factor of 2 better than Variant 1. The apparent main component B_2^a is mainly affected by the support and bearing stiffness, therefore it is not significant for shaft variants comparison. The largest higher-order field harmonic is A_3^a. Its distribution is evaluated in terms of a probability function.

B. Bench design

It may appear reasonable to perform an integrated design of the rotating-coil and its support. But as the coil diameter must be as large as possible for a given magnet aperture, the support must be designed to accommodate a number of different shafts. Therefore, the worst case of a slim coil is considered. Proposed designs are evaluated in terms of measurement errors caused by their vibration. The support displacement must then be related to expected forces, in order to obtain the overall stiffness required to the design.

The design of supporting structures becomes particularly critical when the rotating-coil is mounted on moving stages; the example proposed in this section is indeed motivated by the construction of a versatile rotating-coil bench. The support structure under investigation is required to hold the shaft at 1 m distance from a rigid fixation. The slim coil considered is a bulk-resin coil with a diameter of 50 mm. A summary of the evaluation steps is shown in Fig. 3. For the support structure design, the error of the main component is the most relevant figure of merit. The design process is an iteration of different space-frame layouts. They are made by aluminium profiles, taken from a set of commercially available cross-sections. Magnetic measurement performance is maximized, while keeping the weight of the assembly under a certain value.

IV. EXPERIMENTAL VALIDATION

The experimental validation has two main purposes. The first one is the validation of the FEM model, the second is to identify the limitations of the analytical model. Therefore, previously designed, and readily available shafts have been analyzed. The analytical model presented in [6] was experimentally validated, with the vibration analysis of a simple shaft made of a circular outer shell and a PCB. The experimental campaign presented in this paper investigates another shaft with a more complicated layout. This shaft consists of two beams connected by flexible joints. Three coils are mounted on the inner beam and two on the outer one, as shown in Fig. 4. The shaft is entirely made of epoxy resin, whose mechanical properties are given by the manufacturer. In particular, $E = 23$ GPa, $\rho = 1700$ kg/m^3 and $G = 8.5$ GPa. Cross-section properties are computed approximating the outer
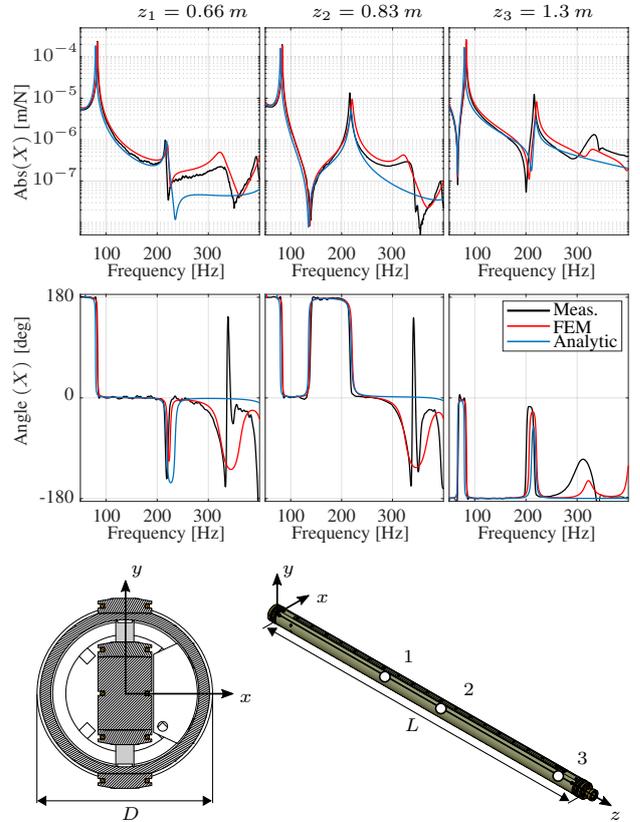

Fig. 4. *The validation of FEM model against the analytical model, for a coil made of a double beam. The response function of three points on the beam are given for an excitation with an impact hammer on point 3. The first to the third bending mode in x direction appears in the spectra. It can be noticed that, above 200 Hz, the analytical model (from [6]) is not able to represent the behaviour of the shaft. The shaft design shown in Fig. is the classical design used at CERN, with $D = 56$ mm and $L = 1360$ mm.*

shell as a hollow cylinder and the inner beam as a rectangular prism. For both geometries, shear correction factors are available [12]. In the most general case, these parameters can be computed also numerically [13]. The main objective is to measure the mechanical vibration modes of the shaft. Two set of measurements are performed, involving both time-domain and frequency domain-signals, for modal analysis [14],[15]. The first one investigates the shaft mounted on an almost ideal elastic supports, the second one on its own bearings. Ideal supports are elastic bands with low stiffness ($2 \cdot 10^3$ N/m, estimated independently), similar to the one in [6]. The system is externally excited by an impact hammer (PCB 086D20) with different tips, mainly one medium tips (-20 dB at 700 Hz) and one hard tips (-20 dB at 1050 Hz). Impacts are provided along x and y axes, to excite modes in both directions. In all the experiments, the system is mounted on an optical table with a tuned mass-damping system. The 3D vibration

spectra of a set of points on the shaft surface is recorded by a 3D vibrometer system (Polytec PSV-400). At least six correct impacts per point are acquired and processed. Model validation is focused on bending modes, but also axial and torsional modes are recorded, to assess that they are not coupled with bending modes.

Moreover, the experimental results are compared with the analytical model, in which the shaft is described as a single beam with equivalent properties. The spectra are shown in Figure 4 up to the third bending mode in x direction. It can be seen that the first two modes are correctly represented by the analytical model, while the following modes require the FEM model.

V. CONCLUSION

The proposed magneto-mechanical model for rotating-coils, expanded in capabilities through FEM formulation, can describe all the main mechanical phenomena affecting magnetic measurements. It has proven to be an effective tool not only for real coil diagnostics but also for predicting the behavior of rotating coils during the design phase. Furthermore, it is possible to assess the design of the supporting structure of the magnetometer. It resulted in the design of the rotating-coil supports for a versatile bench, where the mechanics of the measurement system is particularly critical. The framework here described is easily implementable in optimization routines, and therefore its capabilities in the rotating-coil design are expected to expand in future research.

REFERENCES

[1] S. Russenschuck, Field computation for accelerator magnets, WileyVCH, 2010.

[2] J. Billan, J. Buckley, R. Saban, P. Sievers and L. Walckiers, Design and Test of the Benches for the Magnetic Measurement of the LHC Dipoles, IEEE Transactions on Magnetics, vol. 30, no. 4, July 1994.

[3] N. R. Brooks, L. Bottura, J. G. Perez, O. Dunkel, and L. Walckiers, Estimation of Mechanical Vibrations of the LHC Fast Magnetic Measurement System, IEEE Transactions on Applied Superconductivity, vol. 18, no. 2, June 2008.

[4] G. Tosin, J. F. Citadini, E. Conforti, Long rotating coil system based on stretched tungsten wires for insertion device characterization, IEEE Trans-actions on Instrumentation and Measurement, vol. 57, no. 10, May 2008.

[5] L. Walckiers, Magnetic measurement with coils and wires, CERN Accelerator School: Magnets, Bruges, Belgium 16-25 June 2009.

[6] S. Sorti, C.Petrone, S. Russenschuck and F. Braghin, A Magneto-Mechanical Model for Rotating Coil Magnetometers, Nuclear Instruments and Methods in Physics Research Section A, to be published.

[7] O.Ozsahin, H.N.Ozguven and E.Budak, Analytical modeling of asymmetric multi-segment rotor-bearing systems with Timoshenko beam model including gyroscopic moments. Computer & Structures. 144, November 2014.

[8] G. Genta, Dynamics of Rotating Systems, Springer, 2005 edition

[9] J. Zhou, W. Kang, S. Li, Y. Liu, Y. Liu, S. Xu, X. Guo, X. Wu, C. Deng,290L. Li, Y. Wu, S. Wang, Ac magnetic field measurement using a small flip coil system for rapid cycling ac magnets at the China Spallation Neutron Source (CSNS), Nuclear Instruments and Methods in Physics Research SectionA: Accelerators, Spectrometers, Detectors and Associated Equipment, February 2018

[10] J.N.Reddy, On locking-free shear deformable beam finite elements, Computer Methods in Applied Mechanics and Engineering, 149, October 1997.

[11] S. Russenschuck, G. Caiafa, L. Fiscarelli, M. Liebsch, C. Petrone, P. Rogacki, Challenges In Extracting Pseudo-Multipoles From Magnetic Measurements, 13th Int. Computational Accelerator Physics Conf. ICAP2018, Key West, FL, USA JACoW.

[12] G.R. Cowper, The shear coefficient in Timoshenko beam theory, Journal of Applied Mechanics, vol. 33, June 1966.

[13] F. Gruttmann, W. Wagner, Shear correction factors in Timoshenko beam theory for arbitrary shaped cross-sections, Computational Mechanics, vol. 27, 2001.

[14] H. Van der Auweraer, Structural dynamics modeling using modal analysis:applications, trends and challenges, in: IMTC 2001. Proceedings of the 18th IEEE Instrumentation and Measurement Technology Conference. Re-discovering Measurement in the Age of Informatics, Bucarest, Hungary.

[15] Z. Li, M. J. Crocker, A study of joint time-frequency analysis-based modal analysis, IEEE Transactions on Instrumentation and Measurement, vol. 55, no. 6, January 2007.